Available online at www.CivileJournal.org

Civil Engineering Journal

(E-ISSN: 2476-3055; ISSN: 2676-6957)

Vol. 8, No. 12, December, 2022

Dam-Break Energy of Porous Structure for Scour Countermeasure at Bridge Abutment

Ira Widyastuti [1*], M. Arsyad Thaha [1], Rita Tahir Lopa [1], Mukhsan Putra Hatta [1]

[1] *Department of Civil Engineering, Faculty of Engineering, Universitas Hasanuddin, Makassar 90245, Indonesia.*

Received 26 August 2022; Revised 26 October 2022; Accepted 09 November 2022; Published 01 December 2022

Abstract

The aim of the study is to determine the structure for energy absorption in order to countermeasure the scouring on the bridge abutment. Consider a porous structure for energy absorption, which can reduce flow velocity and depth of scouring due to its porosity. The energy absorber plate demonstrated in triangular shape with several porous as submerged barrier. The investigation was conducted in laboratory and placed the abutment in the middle of the channel with a distance of 3Lb, 5Lb, 7Lb and 9Lb. The plate area consists of 0% (MP1), 5% (MP2), and 10% (MP3). The scour depth measurement (ds) is carried out at 6 crucial points in the abutment area. Comparisons between experimental measurements and a numerical prediction model are presented. The experimental results show that the percentage of frictional velocity in the inhibition area for each pore opening before the obstacle, 31.42% (decreasing), - 9.27% (increasing), and -32.92% (increasing), respectively. Furthermore, the optimum position of the porous energy absorber at 9Lb to the abutment. The magnitude decreases of scour depth obtained from MP2. It can be concluded that the placement of energy absorbers can lead to damping forces. It also found that the porous structures could be beneficial for motion damping and absorber of the scouring.

Keywords: Scouring; Energy Absorber; Velocity; River; Reynolds Number; Froude Number.

1. Introduction

Erosion is one of the river's phenomena that occurs along the channel, which provides an overview of the scouring process and sediment deposition [1]. Scouring is defined as the erosion of a riverbed (vertical scour) or riverbanks (lateral scour) by flowing water. Scour can occur gradually or episodically during floods. Factors that control scour are the river flow, the characteristics of the riverbed and riverbank sediments, and the capacity of the river to transport sediments. This is a natural phenomenon caused by the rate of sediment transfer in the area exceeding the upstream sediment rate. This occurs when the flow velocity in the channel exceeds the velocity at which the base material moves.

In addition, changes in flow patterns are due to the morphology and obstacles that cross the river, such as bridge pillars and abutments, river groves, and sluice gates. They are followed by the local scour around the building [2]. When the flow is separated by immovable obstructions (buildings) in the riverbed area, it will increase scour and sedimentation from the acceleration and deceleration of the flow around the obstacle. Fan et al. (2021) studied porous materials and found that filling them with polymer foams improved energy absorption and shock resistance [3]. Although the porous materials were improved when compressed under densification, strain energy is almost as dynamic. Previous studies have been conducted to countermeasure the scouring [4–9]. Mackay et al. (2021) stated that the scour is not confined to the

* Corresponding author: iwidyastuti09@gmail.com

http://dx.doi.org/10.28991/CEJ-2022-08-12-019

structure; the strength and durability of the structure get into it [8]. Furthermore, Shahsavari et al. (2021) found that the scouring will cause problems when the subsidence of the riverbed causes instability or failure of structures located on or close to the river [5].

Several studies have been investigated the scouring by using model and make an approach simulation to the energy absorption [9, 10]. While, the structure that is generally located on the river is a bridge. Statistical surveys conducted on the investigation of the reasons for bridge failure imply that most of the bridges have failed due to excessive scouring of infrastructure elements during floods [3]. Otherwise, most of the studies often calculated the phenomenon by using a linear wave variable using curtain model as an obstacle to distributed the velocity. The "curtain" model only distributed statically, therefore it is need to conducted a new freshly design for the energy absorber. Subsequently, the most important thing is the combination between statics and dynamics into approaching method to obtain the effective, optimum, and efficient results. In these approaches, the flow through the openings in the porous surface is not modelled explicitly, but is parameterized in terms of a pressure drop as a function of flow velocity, with either a linear or quadratic pressure–velocity relation. Therefore, the effect of the energy damper's distance on the depth of scour of the bridge abutments are important. Consequently, this study aims to obtain the relationship between flow velocity parameters and scour depth due to the presence of porosity structure of an energy damper.

2. Literature Review

2.1. The Scouring Mechanisms around The Abutment

Scouring can occur in bridges if its structure affects the balance between water and the stability of the base material channel. If the bridge has one or more piers that are stream, or if the water level reaches one or both abutments, the structure will affect the flow pattern of the river [8]. The first effect is to reduce the width of the river at the site the bridge is located. For certain flows, this reduction in width will resulted in a rise in the water level upstream of the bridge and increased speed at opening. If this increase in speed causes displacement or movement of the channel bed material, then the bottom surface of the channel around the bridge will decrease. Decrease The bottom surface of this channel is known as general scour. The influence degree of background current and wave on the scour is obtained by comparing the scour hole profile [11]. This statement was highlighted and described in Figure 1. The live- bed occurs when the scour hole is continuously supplied with sediment by approaching stream.

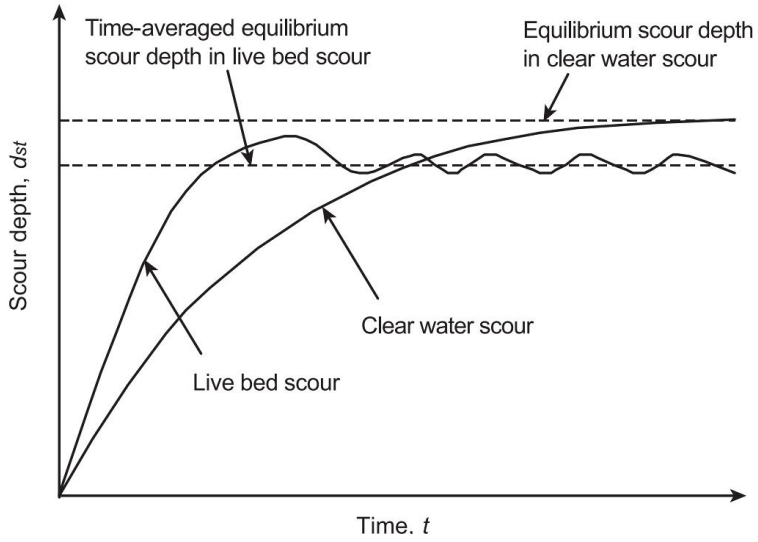

Figure 1. Correlation between scour depth (clear water and live bed scour) with time [12]

Figure 1 shows that there is a good correlation between scour depth and time. It can be seen that the graph clearly assumed that the length of duration influenced the equilibrium scour depth in clear water scour [12]. Time variation of clear-water scour and live-bed scour shown schematically. They may suffer serious threats from long time scour process during constructions and operations. Time factor is crucial to predict this long duration process. However, time factor are mostly proposed for single pile and pipeline, limiting the application effectiveness in pile groups [5, 13]. They focus on scour under threshold velocity intensity and cannot be directly applied in live bed condition.

In rivers with a floodplain, abutment scour becomes much more complex [3]. The Abutment scour is by far more complex than its counterpart associated with piers because of the possibility of the presence of a floodplain. Notwithstanding this, the mechanism of scour at both piers and abutments is very similar; moreover, the failure mechanisms associated with both armoring and flow-altering countermeasures are not very different. The second effect of the interaction between the bridge and the water flow is local disturbance to the flow. This can cause flow acceleration through the bridge piers and increase turbulence, which can result in a decrease in the bottom surface of the channel to

a level that can interfere with the structure of the bridge. The descent of the bottom of this channel is known as local scour [13]. Based on the sediment transport model by the flow approaching, grouping local scour into two categories, namely clear-water scour and live-bed scour. In cases where the abutment ends at or near to the floodplain, it can initiate bank erosion, which clearly is an important erosion problem that is quite distinct from the customary scour at either an abutment in rivers without a floodplain or a pier. For this reason, abutment scour can be very site-specific while pier-scour is more generic in nature. To this end, the ability to identify the type of abutment scour that may form in a particular channel is closely related to an engineer's ability to propose devices for effective scour countermeasure [14-16]. Clear water scour occurs without sediment transport by the oncoming stream flows into the scour hole.

2.2. The Structure of Energy Absorber on The Bridge Abutment

According to Hassan et al. (2020) [17], the scour depth depends on several variables, namely fluid characteristics, base material, flow in the channel and the shape of the pillars or bridge abutments which can be written:

$$d_s = f(\rho, \vartheta, g, d_m, \rho_s, D_0, U, L_b) \quad (1)$$

where ρ is fluid mass density, ϑ is fluid kinematic viscosity, g is acceleration due to gravity, d_m is sediment grain diameter, ρ_s is sediment mass density, D_0 is flow depth, U is average flow velocity, L_b is abutment width. The equation is made dimensionless, then the equation becomes:

$$\frac{d_s}{L_b} = f\left(\frac{u.L_b}{\vartheta}, \frac{U^2}{gL_b}, \frac{D_0}{L_b}, \frac{d_m}{L_b}\right) \quad (2)$$

Due to the characteristics of the flow that passes through the barriers will be difficult to analyze, the empirical approach needs to be taken into account by determining the distribution of flow velocity in the inner region and outer region. In the base region, the speed is controlled by the frictional velocity by obtaining the relationship between u and u*, so the equation becomes:

$$\frac{u}{u^*} = \frac{1}{k} lny + c \quad (3)$$

where u is velocity in the x direction; u* is swipe speed; k is von-karman number; C is constant of integration. The actual velocity distribution can be expressed by the empirical equation:

$$\frac{u\,(z)}{U_m} = \left(\frac{z}{D_m}\right)^{\frac{1}{\alpha_v}} \quad (4)$$

$$\frac{u(z)}{U_m} = exp\left[-\beta_v \left(\frac{z - D_m}{D - D_m}\right)^{\gamma_v}\right] \quad (5)$$

where $u\,(z)$ is average speed z distance from the base; U_m is Maximum flow rate; D_m is High limit of maximum speed ($z = D_m$); β_v is the value of the energy coefficient in the vertical direction; v is the energy momentum coefficient, and v is a value based on the measurement results following an exponential function whose variable is a logarithmic basis. For the outer region, it is controlled by the frictional speed that occurs between the water table boundaries.

The scour control method generally uses riprap, which is placing rocks into the most potential scour holes. Graf (1998) in Dargahi (1990) stated that riprap is the most effective protection to control scour holes by piling rock into the scour with a width of 2-3b and a thickness of 3d [1]. The use of vegetation on the canal bank around the abutment seems well known. The results of the investigation stated that the scour depth can be reduced by 39% compared to cliffs without vegetation [2]. According to Reinaldi (2001), flexible vegetation affects the lift (Cd) and friction (Cf) of the flow velocity [4]. The researcher suggests that (Cd) and (Cf) values are not constant at different depths and vegetative densities. The addition of roughness in the bridge structural elements with variations and combinations of roughness such as the installation of the abutment wall is 0.23 L, giving an artificial groove where the results state that more than 25% of the local scour of the abutment will be reduced and the combination of collar plate installation and manufacture coarse grooves will reduce local scour by 83% [10, 12, 18].

In addition, Wilson et al., (2022) conducted a study in the form of using poles that were installed upstream of the abutment and showed that the maximum pile position at the foot of the bank would reduce scour by 26.58% [15]. It was shown that the obstacle causes the distribution of turbulent kinetic energy of the flow to be modified significantly such that at its downstream the turbulent intensity profiles appears to have a non-uniform distribution over height. Also it was shown that the turbulent kinetic energy has larger magnitude at obstacle's downstream. In addition, in the presence of the obstacle the variation of the local Froude number seems to be more significant over the height at its downstream which is compatible with the changes in turbulent kinetic energy. Moreover, it was quantitatively confirmed that in the absence of the obstacle, as the inlet Froude number increase as from subcritical to the supercritical flow, the turbulent intensities along the channel seem to increase.

3. Research Methodology

The experimental work was conducted at Hidrology Laboratory, Universitas Hasanuddin, Gowa, South Sulawesi, Indonesia. The material used as the base sampling is uniform sand taken from the Jeneberang River, Gowa, South

Sulawesi, Indonesia. The coordinate of sampling site is 05º 10' 00"- 05º 26' 00" S and 119º 23' 50"-119º 56' 10" E. The data collection and design modelling for the energy absorber during the investigation process. The schematic of an open channel is shown in Figure 2.

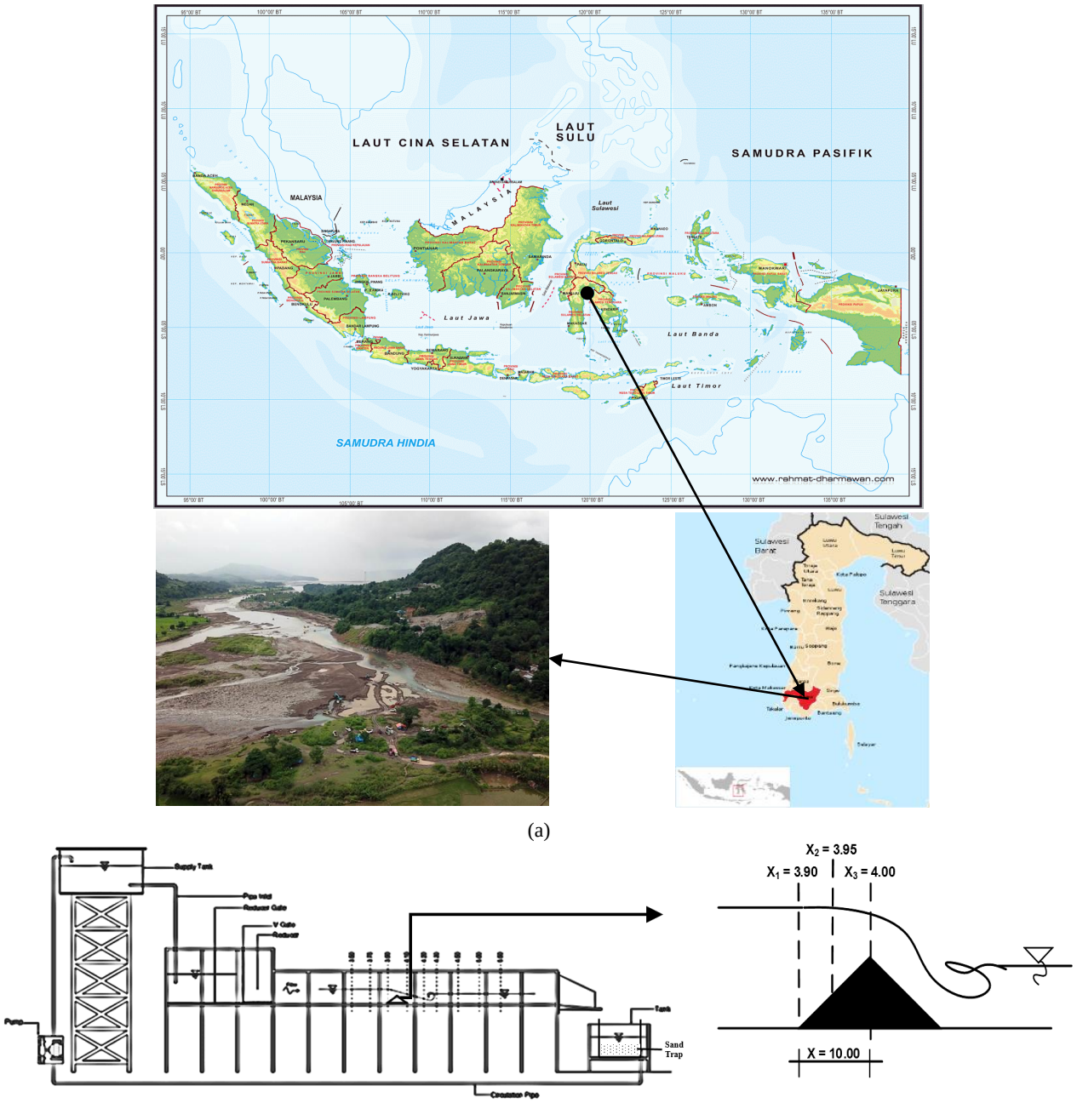

Figure 2. (a) Sand sampling location in Jeneberang River, South Sulawesi, Indonesia; (b) The Schematic of an open channel

Figure 2 explain that the flow energy will be damped by the frictional resistance of the channel horizontally. If the obstacle placed at the bottom of the channel, it can cause a speed reduction but will increase the direction flowability [19-24]. Therefore, the schematic will lead to design an efficient energy absorber model to inhibit the flow velocity. A porous structure energy absorber is applied to be obstacle. It was design in a triangular plate shape with various pores as shown in Figure 3.

Figure 3 explain the way to measure depth and velocity in description. The plate was placed at 0.6D from the average water level which is ± 10.90 cm from the bottom of the channel. The height of plate is 6.00 cm with a pore variation to the plate area are 0% (MP1), 5% (MP2), and 10% (MP3), respectively. They are placed at a distance of x = 4.00 m from the inlet with 24h flow velocity readings. Furthermore, the distance can be changed to x1 = 3.50; x2 = 3.90 m; x3 =3.95 m; x4 = 4.00 m; x5 = 4.25 m; x6 = 4.50 m; x7 = 5.00 m, and x8 = 5.50 m at the base slope. The channel is open in the upstream boundary conditions approximately 11.00 cm and downstream boundary conditions is 8.00 cm. For measuring flow velocity using ADV and scouring depth with a point gauge. The flow chart of the experimental works is shown in Figure 4.

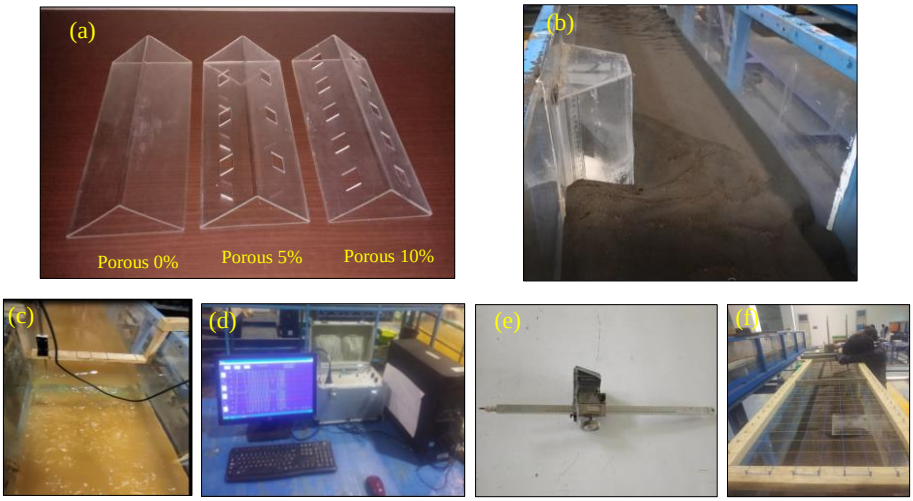

Figure 3. (a) Model of Porous energy dam-break; (b) Wing wall abutment bridge type; (c) and (d) 2D electromagnetic current meter; (e) and (f) Point gauge measurement

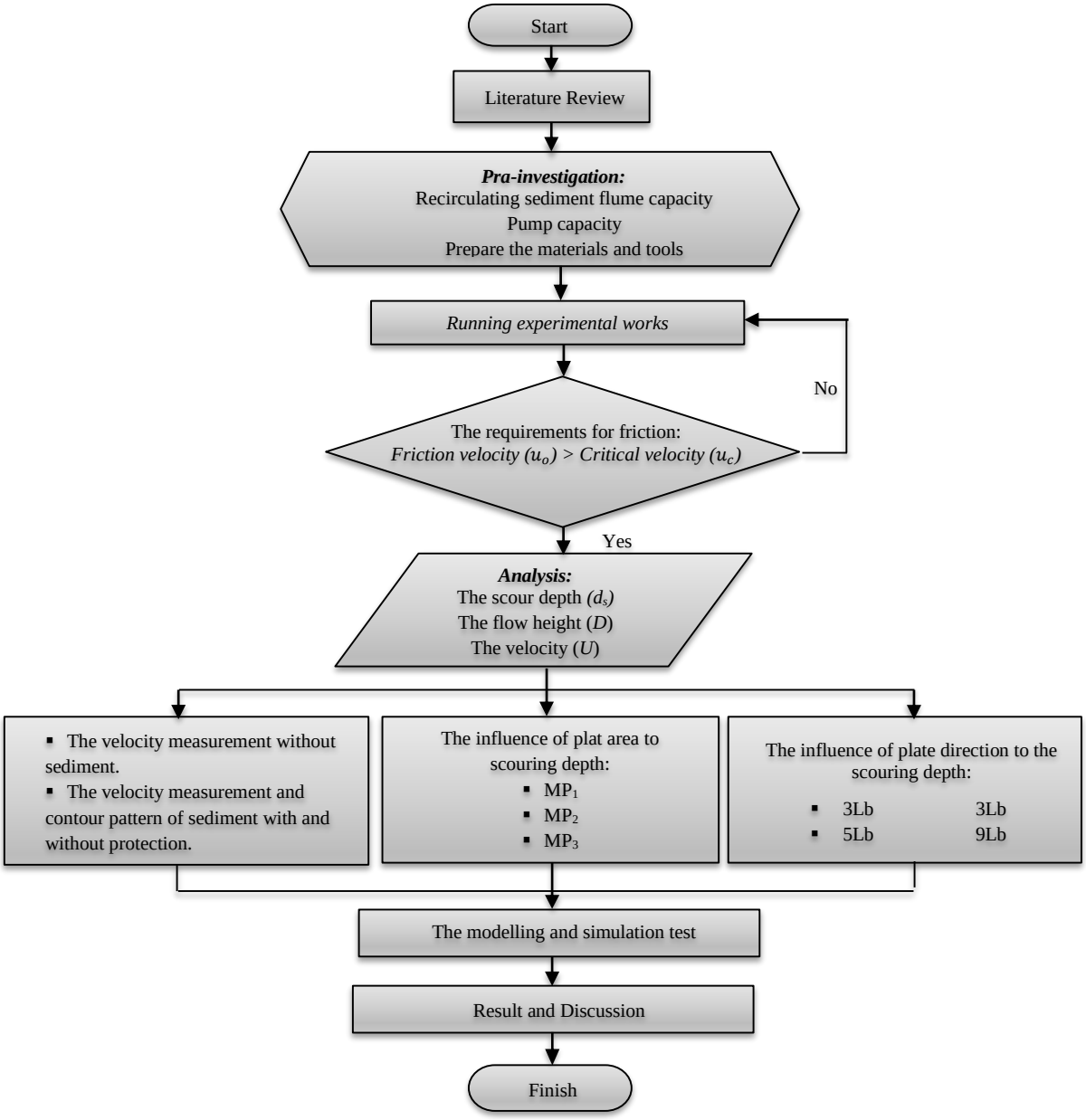

Figure 3. The flow chart of the experimental works

4. Result and Discussions

4.1. The Distribution of Velocity Flow Pattern in the Porous Structure of an Energy Damper

The results of the division of the velocity area ratio and velocity distribution (Uz) based on the area whose measurements were made in the middle of the span (X = 3.75 m and X = 4.25 for MP1) can be seen in Table 1 and the distribution results for each porous barrier are in Figure 5. Table 1 as a sample of measurement (MP1) which is simply shows the way to measure the flow distribution based on regional division. It also measures the flow pattern inner and outer region. This result in line with the previous study which explained that the velocity area will have 2 main regions, they are inner and outer region [21, 24, 25]. The inner and outer region have equation to measure, they are Equations 4 and 5.

Table 1. Distribution of flow velocity based on area division

Flow Pattern	MP 1			Velocity Area								
	X=3.75			z/D_m	γ_u	$\beta = \frac{\sum v^2 \Delta A}{v^2 \Delta A}$	$\alpha = \frac{\sum v^3 \Delta A}{v^3 \Delta A}$	Inner region	Outer region	$\frac{U_z}{U_z}$	U_z	
	Z	D	U					$u(z)/Um = \left(\frac{z}{Hm}\right)^{\frac{1}{\alpha}}$	$u(z)/Um = exp(-\beta_v \frac{z-Hm}{(H-Hm)^n}$			
$\frac{Z}{D_m}$	0.50	11.20	20.02	0.167			7.282	0.782		0.782	25.958	
	1.00	11.20	21.92	0.333			9.104	0.886		0.886	29.426	
	1.50	11.20	27.38	0.500			16.881	0.960		0.960	31.864	
	2.00	11.20	29.31	0.667			19.636	0.980		0.980	32.522	
Z-D_m	3.00	11.20	33.20	1.000 0.000			25.442	1.000	1.000	1.000	33.200	
	4.00	11.20	18.86	0.139	1	0.217			0.970	0.970	32.214	
	5.00	11.20	36.18	0.323		0.688			0.801	0.801	26.591	
$\frac{Z-D_m}{D-D_m}$	6.00	11.20	20.55	0.577		0.186			0.898	0.898	29.819	
	7.00	11.20	36.18	0.952		0.466			0.641	0.641	21.297	
	8.00	11.20	23.63	1.563		0.152			0.789	0.789	26.202	
	9.00	11.20	22.37	2.727		0.093			0.775	0.775	25.740	
Average U			**26.33**								**28.62**	

Figure 5 shows that the velocity distribution that occurs in the channel before passing through the obstacle will experience an increase in the water level (D) from 9.50 cm to 10.90 cm and result in a decrease in the flow velocity in the bottom area of the channel. This can be seen in Figure 5-b, the inner region experiences a gentle curve (α) at a distance of x = 3.75 m and decreases at the bottom and indicates the average value of slowing speed. It can also be seen in Figure 5-c that the distance x = 4.25 (after passing the plate) is 25.00 cm from the plate axle, a reverse momentum occurs, the flow velocity increases and a hydraulic jump occurs, resulting in an increase in the value of and the flow velocity (U) will start experience a momentary increase to the surface of the flow so that turbulent flow is created in the outer region. As can be seen that MP2 is an effective direction to get an optimum flow distribution using obstacles.

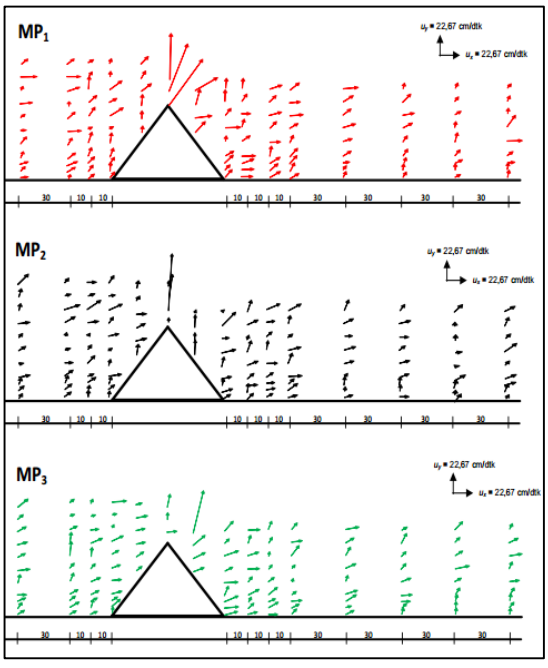

(a)

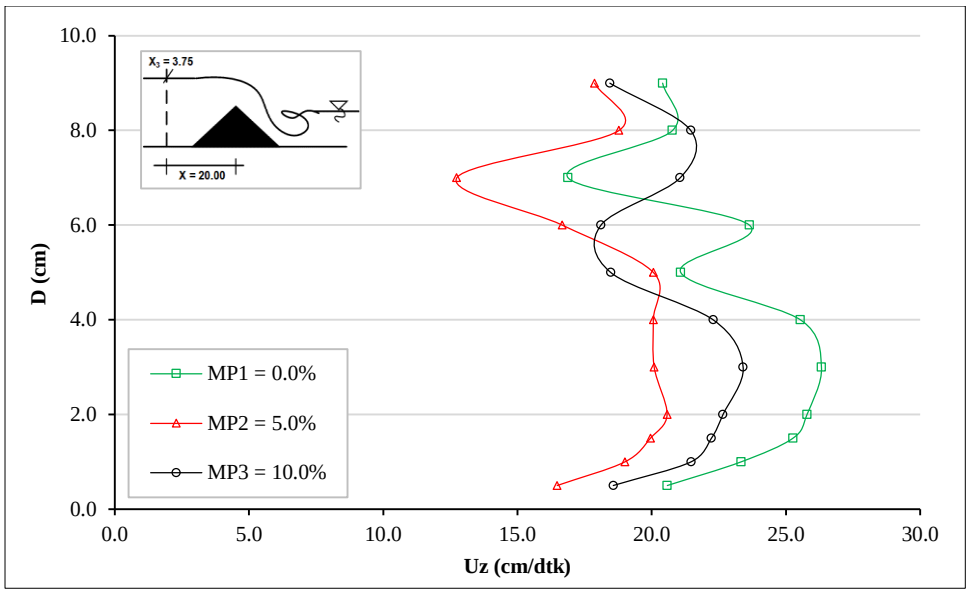

(b)

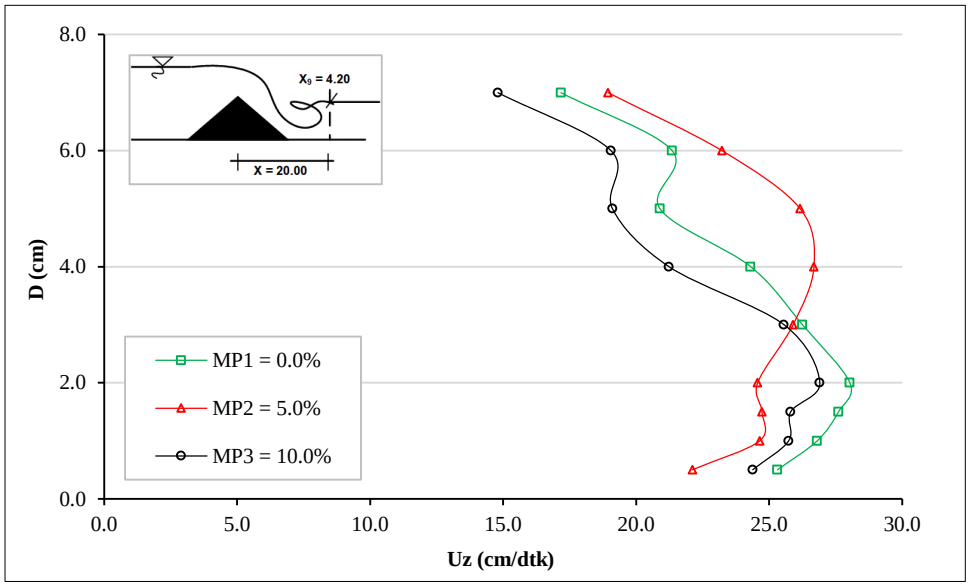

(c)

Figure 4. (a) Velocity distribution at obstacle; (b) Stream velocity distribution (U) before obstacle; (c) Stream velocity distribution (U) after obstacle

Figure 6 shows that the change in frictional velocity (u*) that occurs will be inversely proportional to the constant of integration (C). The value of the frictional velocity (u*) will enlarge to the value of the frictional velocity under normal conditions (u*L) so that the flow will slow down (MP1) in the upstream area of the obstacle, this is because the resistance will restrain the flow rate which indicates the ability of the flow to require greater energy to back to normal flow. However, due to the pore openings (MP2 and MP3), the flow in the upstream area slowly increases along with the pore openings, indicated by the value of the frictional velocity (u*) will decrease which indicates that due to the presence of pore openings, the flow velocity will increase. This condition is inversely proportional to when the flow passes through the obstacle, where the flow will momentarily increase the flow rate, but when it moves away from the obstacle, the flow will return to normal conditions. In Addition, if x < 4.00 m (MP1), experiencing a change in friction velocity (u*) will increase by an average of 31% (friction speed (u*p) decreases), whereas if x > 4.00 m, after the flow passes through the obstacle to the friction speed value will decrease (friction speed (u*p) increases) by an average of 37%. M. Kordaneij et al., (2017) stated that the obstacles will be a spam in the river area when placed properly [25]. However, the frictional velocity trend shown for the pore opening model shows that the flow before passing through the obstacle will decrease with the percentage of pore openings in the model. Likewise, when the flow passes through the barriers in the MP1 and MP3 models, the percentage of flow velocity increases significantly, namely 37% and 43%, while in the MP2 model the smallest increase in flow velocity is 25%. It can be concluded that the porosity affected the frictional velocity as well as flow distribution both in longitudinal or transversal.

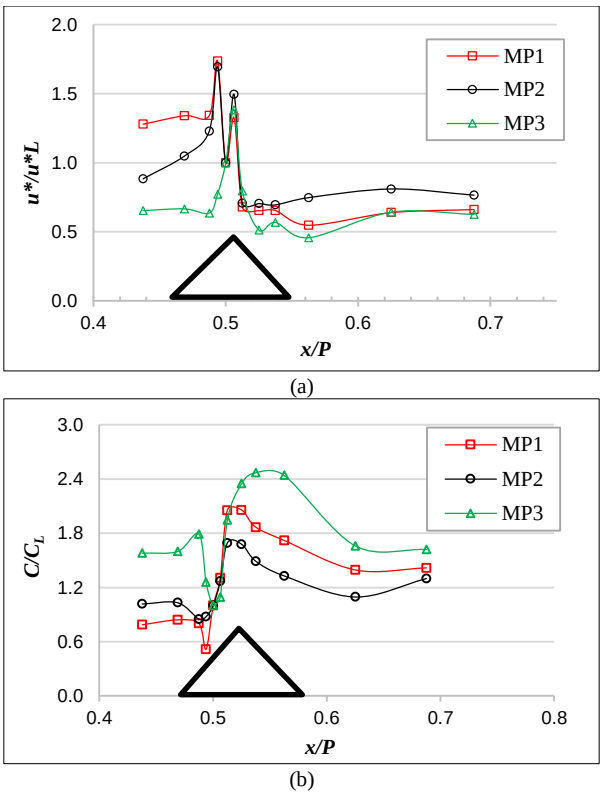

Figure 5. The effect of the porous energy absorber structure on the distribution of a) u*/u*L and b) C/CL with x/P in the longitudinal direction

4.2. The Flow Characteristics and Scour Pattern in The Abutment

The analysis shows the comparison of the frictional velocity value under normal conditions (u^*) with the critical shear velocity (u_{*cr}) in the inner region where $u^* < u_{*cr}$, then it can be said that the basic grain does not move. The average speed under normal conditions (U*) is smaller than the average critical speed (U_{cr}) or $U < U_{cr}$, so it can be concluded that the scour that occurs in the area around the abutment is a clear water scour. The flow characteristics are shown in Table 2. The *Fr* value both in Critical and Normal Depth is 0.2 and categorized as fulfilling the requirements [3, 8, 14, 16].

Table 2. The Flow Characteristics

Critical Depth (Dcr = 9,50 cm)			Normal Depth (Do = 10.90 cm)		
Notation	**Unit**	**Value**	**Notation**	**Unit**	**Value**
Q	m^3/s	0.010	*Q*	m^3/s	0.010
Ucr	m/s	0.297	*U*	m/s	0.242
Fr	(-)	0.271	*Fr*	(-)	0.218
u_{*cr}	cm/s	2.626	u^*	cm/s	2.132
C	(-)	7.979	*C*	(-)	10.427

The transported sediment will be carried by high flow velocities until the sediment is deposited. Figure 7 shows that the aggradation occurs in the downstream right to the abutment. It will stop if flow conditions return back to normal. With regards to the utilization of obstacles for flow velocity control, some investigations have been performed in the literature. For example, Oehy & Schleiss (2007) examined the placement of an obstacle before a reservoir to control the sedimentation [16]. Their findings show that scouring could be affected well by appropriately designed constructive measures. Meiburg & Kneller [26] reviewed some studies on the structure and scouring phenomena, saying that when sediment gravity flows face with the topography which is not completely flat, the topography influences deposition significantly. Therefore, it is also important to reveal how such barriers affect the absorber structure of the flow since the scouring could influence the deposition behavior (e.g., Sediment Resuspension) [27]. As this effect has been explored very systematically, and also capable of measuring the instantaneous velocity at each point with and without protection.

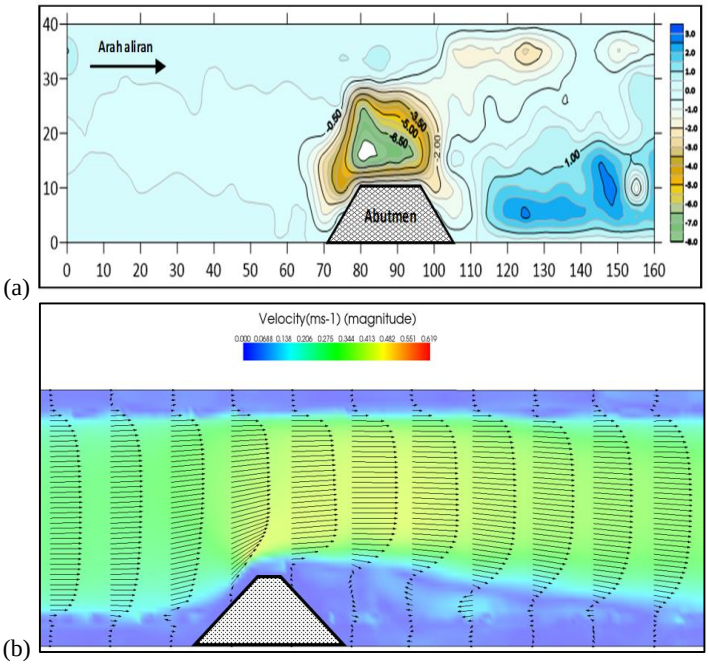

Figure 7. (a) Scour pattern in unprotected abutments; and (b) Flow velocity distribution profile in clear water scour conditions

In the downstream (side) abutment, the flow velocity tends to be slow and rotating (vortex), but the energy generated is not large so that the scour that occurs tends to be deposited locally and there will be aggradation around the downstream of the abutment. Maximum scour depth that occurs in clear water conditions the scour for unprotected wingwall abutments is at point 3, while at point 6 there is a tendency for silting to occur as shown in Figure 8, in the form of depth of scour development based on time.

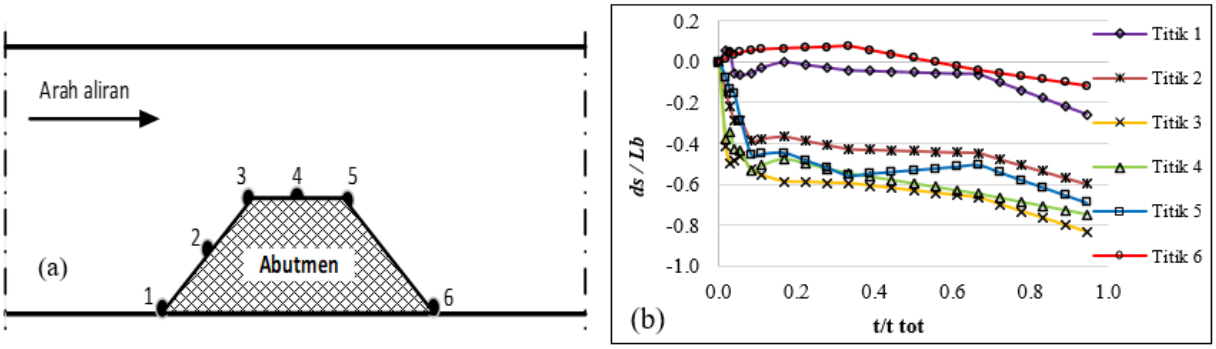

Figure 6. (a) Scour depth review point and (b) Relationship (t/t total) with (ds/Lb) clear water scour conditions at 6 (six) observation points

4.3. The Flow Characteristics and Scour Patterns in Bridge Abutments with Protection

The flow characteristics and scour patterns is important to calculated the optimum distance between absorber and the abutment axle. As the beginning of the research on the depth of scour in the abutment, primarily conducted simulation to reduce the scour depth before protection and get the most optimum scour depth. Figure 9 described the flow pattern and the depth reduction caused by the patterns. To obtain the optimum distance, observations were made at the maximum time, namely the occurrence of the scour regime at the 3 (three) observation points in the abutments.

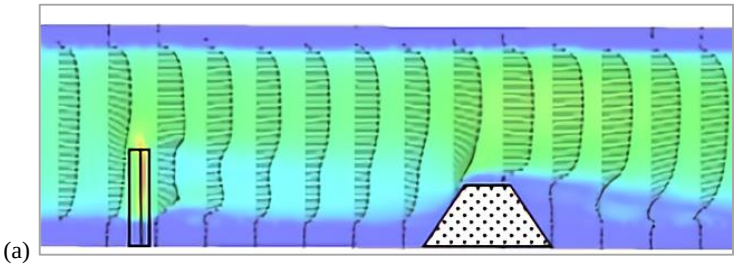

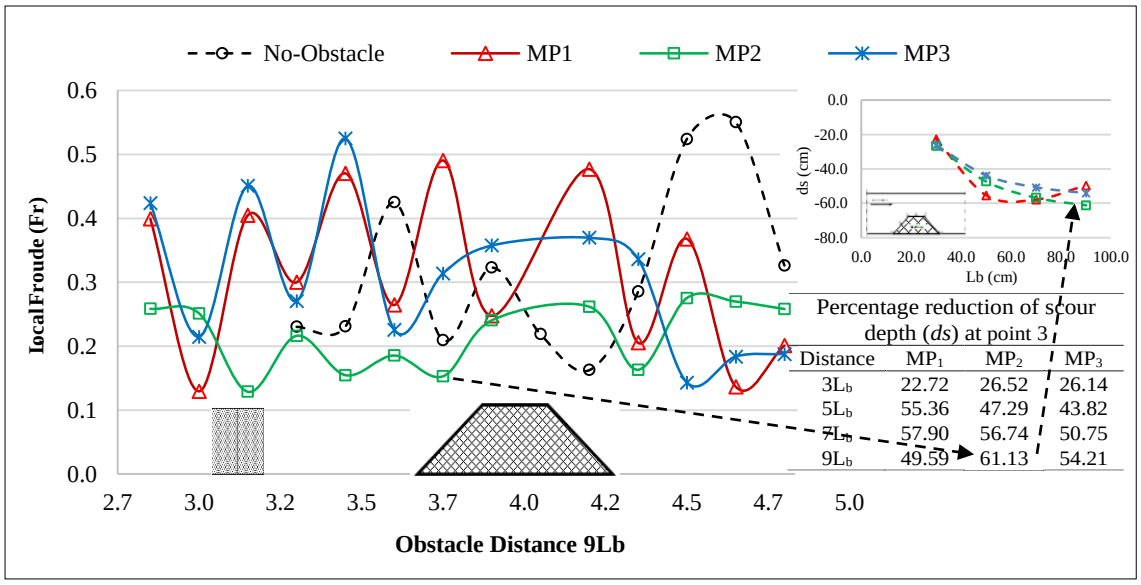

(b)

Figure 7. (a) Velocity distribution profile in abutments due to MP1 resistance and (b) Graph of reduction in scour depth due to resistance to distance at the deepest point (Point 3)

The flow pattern that occurs around the abutment is due to the flow velocity created by the energy absorber structure at a distance of 3Lb to 9Lb (Figures 10). The turbulent flow that occurs momentarily through the obstacle will lift the bottom sediment and the sediment will be deposited not far from the structure area which in turn causes the flow velocity to decrease and tend to have the same magnitude at the front of the abutment. At the downstream side (next to the abutment) there will be a vortex (turbulent) flow but it has a small energy which causes aggradation. The protection (barriers) placed at each distance will contribute to the depth of scour around the energy absorber structure and degradation downstream of the abutment, in addition, degradation also occurs downstream of the barrier structure due to pore holes in the structure. Porous materials are often used in marine structures to dissipate wave energy and reduce wave heights around a structure [7]. The flow through the porous surface is subject to both viscous drag and turbulent dissipation of energy. It is assumed that the wakes are quickly homogenized into the flow within a short distance of the porous surface. However, the flow velocity formed after passing through the damper structure will affect the depth of scour that occurs around the abutment.

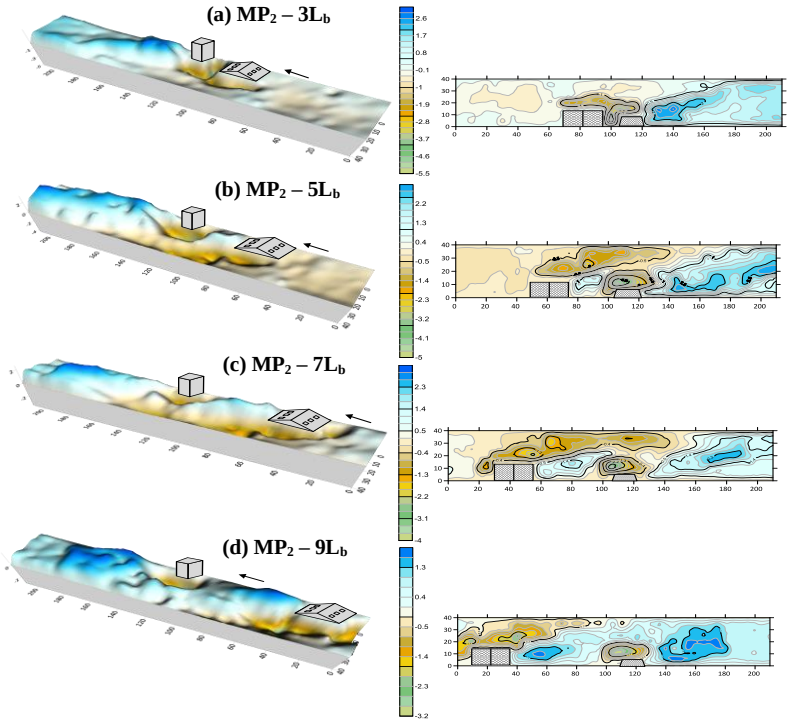

Figure 8. The scour pattern at each protection distance with clear water scour conditions

Reynolds and Froude relationship shows two variables which from experimental data show a non-linear trend. Non-linear regression is generally based on a function (mean value) which is assumed to be nonlinear with indefinite coefficients that will be calculated from observational data, so the non-linear regression equation becomes:

$$E(Y/x) = \alpha + \beta\ ln(x) \tag{7}$$

As for the results of the calculation of multiple non-linear regression, then the equation is obtained:

$$\frac{d_s}{L_b} = 3.836 + 3.978.10^{-5}\left(\frac{U\,L_b}{\vartheta}\right) - 65.698\left(\frac{U^2}{g\,L_b}\right) \tag{8}$$

Figure 11 shows 2 (two) flow characteristics that affect the scour depth and has almost the same graph. The Reynolds number that occurs slightly dominates the flow around the abutment, this can be seen from the trendline trend that is up and describes the turbulent level in the abutment area, where the greater the Reynolds and Froude values, the greater the depth of scour that occurs in the abutment.

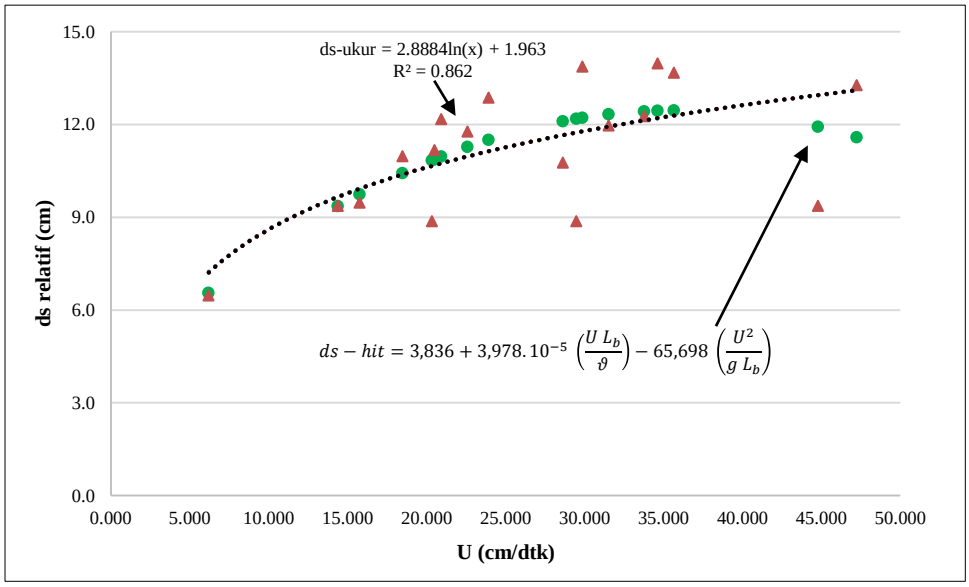

Figure 9. Relationship of flow velocity (U) due to porous SPE to relative scour depth in clear water scour conditions

Figure 11 explained the relationship between flow velocity and scouring depth. The variables that influence the wave reflection are the depth of the water, the height, and the length of the wave. The scouring absorber that has the smallest reflection coefficient is the MP2. It is a model in which the energy absorber was placed at the optimum distance is 9Lb and due to the structure of the energy absorber, which has many porous on its surface. The diagonal line in the graph represents a composite of the results, with and without obstacles. As can be seen, the direction of the arrow points close to MP2. It is due to the distance of the obstacle placement and the porous structures. Subsequently, the most effective model that can reduce the scour in the abutment is MP2. It is evident from the previous gap that the triangular porous structure is a proper model to design such an energy absorber in the river. The MP2 produces an optimal result due to the placement of the obstacle and the abutment distance. It is also strengthening that most of the former curtain model, which was placed near the embankment, is not effective in the flow distribution analysis. It is suggested to use triangular porous energy absorbers to effectively decrease the depth of scouring near the abutment. As a conclusion, the porous structure of an energy absorber will lead to a decrease in the depth of scouring at the bridge abutment.

5. Conclusion

The simulation validates the variation effects of the porous structure energy absorber (MP1, MP2, and MP3) on flow velocity before passing through the obstacle. The results show that the flow velocities obtained are 31.42% (decreasing), - 9.27% (increasing) and -32.92% (increasing), respectively. While the flow velocity after passing through the obstacle will experience a significant increase in the mean flow velocity which is gained up to -37.80%, - 25.00 and -43, respectively. It can be said that the porous structure of an energy absorber will properly work depending on the flow velocity, contact area (A), the width of the abutment, and gravity. The optimum position of the porous energy absorber is at 9Lb to the abutment. The magnitude decreases of scour depth obtained from MP2. It can be concluded that the placement of energy absorbers can lead to damping forces. It also found that the porous structures could be beneficial for motion damping and absorber of the scouring.

6. Declarations

6.1. Author Contributions

Conceptualization, I.W and M.A.T.; methodology, I.W.; software, I. W.; validation, M.A.T., R. T. L and M.P.H..; formal analysis, I.W.; investigation, I.W.; resources, I.W.; data curation, I.W.; writing—original draft preparation, I. W.; writing—review and editing, I.W.; visualization, I.W.; supervision, M.A.T., R.T.L and M.P.H.; project administration, I.W.; funding acquisition, I.W. All authors have read and agreed to the published version of the manuscript.

6.2. Data Availability Statement

The data presented in this study are available on request from the corresponding author.

6.3. Funding

The authors received no financial support for the research, authorship, and/or publication of this article.

6.4. Acknowledgements

I would like to say thank you for all the support from supervisors, staff, laborers, and colleagues. Through ups and downs, they are still beside me, strengthening my willingness to finish this study on time.

6.5. Conflicts of Interest

The authors declare no conflict of interest.

7. References

[1] Dargahi, B. (1990). Controlling Mechanism of Local Scouring. Journal of Hydraulic Engineering, 116(10), 1197–1214. doi:10.1061/(asce)0733-9429(1990)116:10(1197).

[2] Llewellyn, R. J., Yick, S. K., & Dolman, K. F. (2004). Scouring erosion resistance of metallic materials used in slurry pump service. Wear, 256(6), 592–599. doi:10.1016/j.wear.2003.10.002.

[3] Fan, Z., Zhang, B., Liu, Y., Suo, T., Xu, P., & Zhang, J. (2021). Interpenetrating phase composite foam based on porous aluminum skeleton for high energy absorption. Polymer Testing, 93, 106917. doi:10.1016/j.polymertesting.2020.106917.

[4] Rinaldi, B. Y. (2001). Physical Model of Scour Control around Bridge Abutments. Forum Teknik Sipil, X, 139–149. (In Indonesian).

[5] Shahsavari, H., Heidarpour, M., & Mohammadalizadeh, M. (2017). Simultaneous effect of collar and roughness on reducing and controlling the local scour around bridge abutment. Acta Universitatis Agriculturae et Silviculturae Mendelianae Brunensis, 65(2), 491–499. doi:10.11118/actaun201765020491.

[6] Abdurrosyid, J., & Fatchan, A. K. (2007). Scour Around the Abutments and Its Control in Existing Transport Conditions for Multiple Channels. Dinamika Teknik Sipil, 7(1), 20–29. (In Indonesian).

[7] Mackay, E., Shi, W., Qiao, D., Gabl, R., Davey, T., Ning, D., & Johanning, L. (2021). Numerical and experimental modelling of wave interaction with fixed and floating porous cylinders. Ocean Engineering, 242, 110118. doi:10.1016/j.oceaneng.2021.110118.

[8] Mackay, E., Liang, H., & Johanning, L. (2021). A BEM model for wave forces on structures with thin porous elements. Journal of Fluids and Structures, 102, 103246. doi:10.1016/j.jfluidstructs.2021.103246.

[9] Krishnendu, P., & Balaji, R. (2020). Hydrodynamic performance analysis of an integrated wave energy absorption system. Ocean Engineering, 195, 106499. doi:10.1016/j.oceaneng.2019.106499.

[10] Amir, M. U. A. R., Hashmi, H. N., Baloch, M., Ehsan, M. A., Muhammad, U., & Ali, Z. (2018). Experimental investigation of channel bank vegetation on scouring characteristics around a wing wall abutment. Technical Journal, 23(01), 15-21.

[11] Zhao, E., Dong, Y., Tang, Y., & Sun, J. (2021). Numerical investigation of hydrodynamic characteristics and local scour mechanism around submarine pipelines under joint effect of solitary waves and currents. Ocean Engineering, 222, 108553. doi:10.1016/j.oceaneng.2020.108553.

[12] Pu, J. H., Hussain, A., Guo, Y. kun, Vardakastanis, N., Hanmaiahgari, P. R., & Lam, D. (2019). Submerged flexible vegetation impact on open channel flow velocity distribution: An analytical modelling study on drag and friction. Water Science and Engineering, 12(2), 121–128. doi:10.1016/j.wse.2019.06.003.

[13] Radice, A., & Davari, V. (2014). Roughening Elements as Abutment Scour Countermeasures. Journal of Hydraulic Engineering, 140(8), 6014014. doi:10.1061/(asce)hy.1943-7900.0000892.

[14] Juez, C., & Navas-Montilla, A. (2022). Numerical characterization of seiche waves energy potential in river bank lateral embayments. Renewable Energy, 186, 143–156. doi:10.1016/j.renene.2021.12.125.

[15] Wilson, R. I., Friedrich, H., & Stevens, C. (2018). Flow structure of unconfined turbidity currents interacting with an obstacle. Environmental Fluid Mechanics, 18(6), 1571–1594. doi:10.1007/s10652-018-9631-7.

[16] Oehy, C. D., & Schleiss, A. J. (2007). Control of turbidity currents in reservoirs by solid and permeable obstacles. Journal of Hydraulic Engineering, 133(6), 637-648. doi:10.1061/(ASCE)0733-9429(2007)133:6(637).

[17] Hassan, Z. F., Karim, I. R., & Al-Shukur, A. H. K. (2020). Effect of interaction between bridge piers on local scouring in cohesive soils. Civil Engineering Journal (Iran), 6(4), 659–669. doi:10.28991/cej-2020-03091498.

[18] Li, H., Barkdoll, B., & Kuhnle, R. (2005). Bridge Abutment Collar as a Scour Countermeasure. Impacts of Global Climate Change. doi:10.1061/40792(173)395.

[19] Ansari, S. A., Kothyari, U. C., & Ranga Raju, K. G. (2002). Influence of cohesion on scour around bridge piers. Journal of Hydraulic Research, 40(6), 717–729. doi:10.1080/00221680209499918.

[20] Igarashi, T. (1981). Characteristics of the Flow Around Two Circular Cylinders Arranged in Tandem - 1. Bulletin of the JSME, 24(188), 323–331. doi:10.1299/jsme1958.24.323.

[21] Gao, Yangyang, Stephane Etienne, Xikun Wang, and Soon Keat Tan. "Experimental Study on the Flow around Two Tandem Cylinders with Unequal Diameters." Journal of Ocean University of China 13, no. 5 (July 9, 2014): 761–770. doi:10.1007/s11802-014-2377-z.

[22] Tafarojnoruz, Ali, Roberto Gaudio, and Francesco Calomino. "Bridge Pier Scour Mitigation under Steady and Unsteady Flow Conditions." Acta Geophysica 60, no. 4 (April 28, 2012): 1076–1097. doi:10.2478/s11600-012-0040-x.

[23] Briaud, Jean-Louis. "Scour Depth at Bridges: Method Including Soil Properties. I: Maximum Scour Depth Prediction." Journal of Geotechnical and Geoenvironmental Engineering 141, no. 2 (February 2015): 04014104. doi:10.1061/(asce)gt.1943-5606.0001222.

[24] Yaghoubi, S., Afshin, H., Firoozabadi, B., & Farizan, A. (2017). Experimental Investigation of the Effect of Inlet Concentration on the Behavior of Turbidity Currents in the Presence of Two Consecutive Obstacles. Journal of Waterway, Port, Coastal, and Ocean Engineering, 143(2). doi:10.1061/(asce)ww.1943-5460.0000358.

[25] Kordnaeij, M., Asghari Pari, S. A., Sajjadi, S. M., & Shafai Bajestan, M. (2017). Experimentally Comparisons of the Effect of Porous Sheets and Porous Obstacles in Controlling Turbidity Current. Water and Soil Science, 27(1), 43-54.

[26] Meiburg, E., & Kneller, B. (2010). Turbidity Currents and Their Deposits. Annual Review of Fluid Mechanics, 42(1), 135–156. doi:10.1146/annurev-fluid-121108-145618.

[27] Asghari Pari, S. A., Kashefipour, S. M., & Ghomeshi, M. (2017). An experimental study to determine the obstacle height required for the control of subcritical and supercritical gravity currents. European Journal of Environmental and Civil Engineering, 21(9), 1080–1092. doi:10.1080/19648189.2016.1144537.